Supporting Information

Structure-based Design and Development of Chemical Probes Targeting Putative MOR-CCR5 Heterodimers to Inhibit Opioid Exacerbated HIV-1 Infectivity

Boshi Huang,[†] Huiqun Wang,[†] Yi Zheng,[†] Mengchu Li,[†] Guifeng Kang,[†] Victor Barreto-de-Souza,[‡] Nima Nassehi,[‡] Pamela E. Knapp,[‡,&] Dana E. Selley,[‡] Kurt F. Hauser,[‡,&] Yan Zhang [†,*]

[†] Department of Medicinal Chemistry, Virginia Commonwealth University, 800 E. Leigh Street, Richmond, Virginia 23298, United States

[‡] Department of Pharmacology and Toxicology, Virginia Commonwealth University, 410 North 12th Street, Richmond,

Virginia 23298, United States

[&] Department of Anatomy and Neurobiology, Virginia Commonwealth University, 1101 E. Marshall Street, Richmond,

Virginia 23298, United States

* To whom correspondence should be addressed. Phone: 804-828-0021. Fax: 804-828-7625. E-mail: yzhang2@vcu.edu

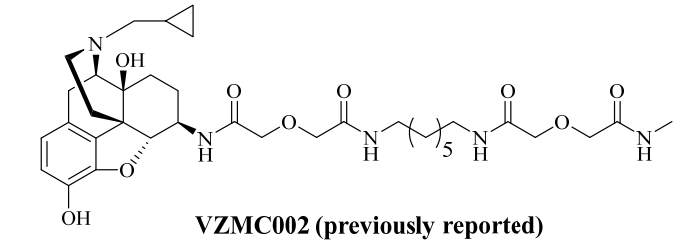

VZMC002 (previously reported)

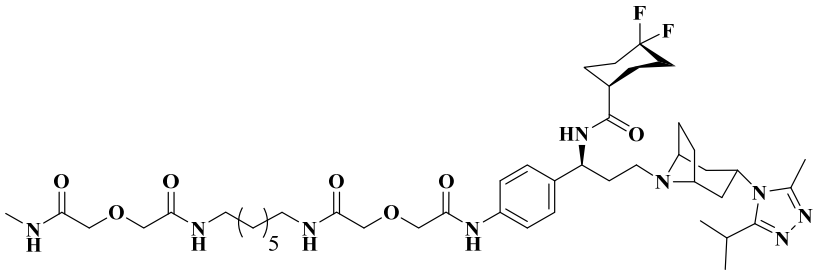

VZMC003 (previously reported)

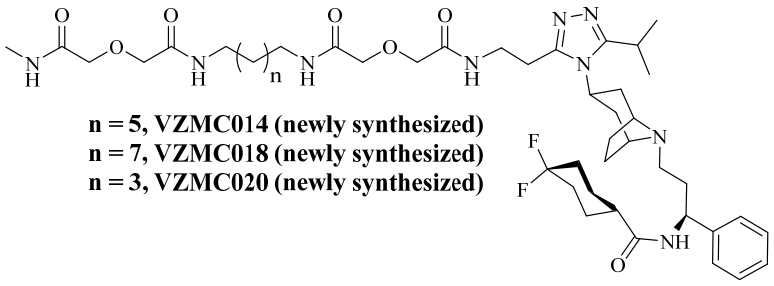

n = 5, VZMC014 (newly synthesized)
n = 7, VZMC018 (newly synthesized)
n = 3, VZMC020 (newly synthesized)

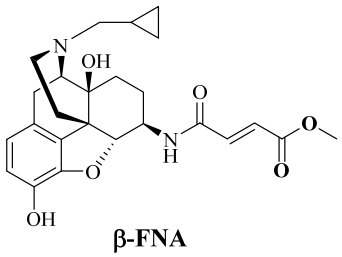

β-FNA

Figure S1. Chemical structures of corresponding bivalent ligands and monovalent control ligands and β-FNA.

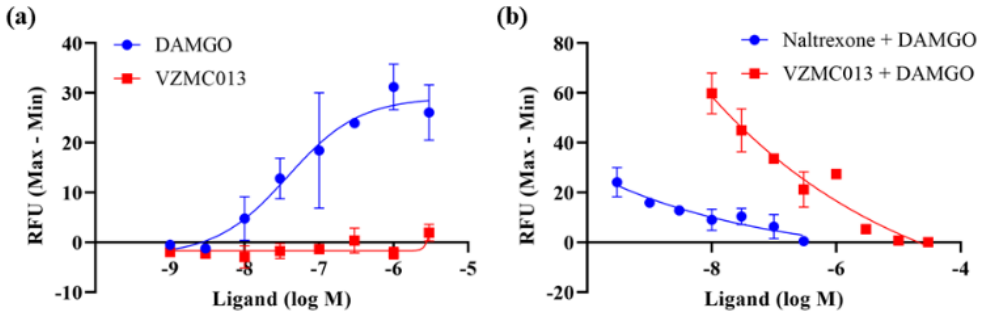

Figure S2. Effects of bivalent compound **VZMC013** on DAMGO-induced Ca^{2+} mobilization in Gqi5-transfected mMOR-CHO cells. (a) **VZMC013** exhibited no agonism to increase the intracellular calcium level. DAMGO was used as a control. (b) **VZMC013** dose-dependently antagonized the DAMGO-induced intracellular calcium increase. Naltrexone was used as a control.

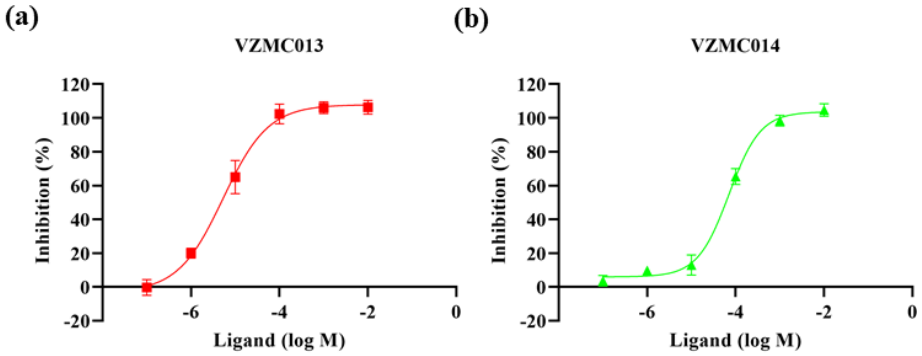

Figure S3. CCR5 Inhibition (%) corresponds to the ability of a tested compound to displace the radiolabeled ligand. (a) The competitive radioligand binding curve of **VZMC013**. (b) The competitive radioligand binding curve of **VZMC014**.

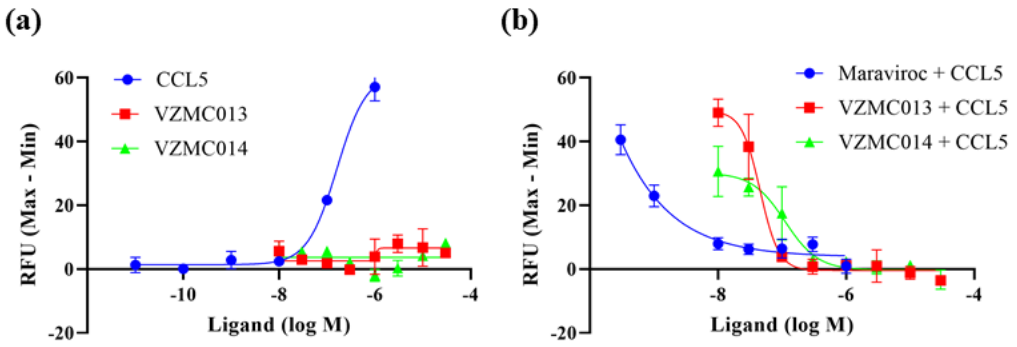

Figure S4. Effects of bivalent compound **VZMC013** and monovalent compound **VZMC014** on CCL5-induced Ca^{2+} mobilization in Gqi5-transfected HOS-CCR5 cells. (a) **VZMC013** and **VZMC014** failed to increase the intracellular calcium levels, suggesting a complete lack of agonist properties at CCR5. CCL5 was used as a control. (b) **VZMC013** and **VZMC014** dose-dependently antagonized CCL5-induced intracellular calcium increases. Maraviroc was used as a control.

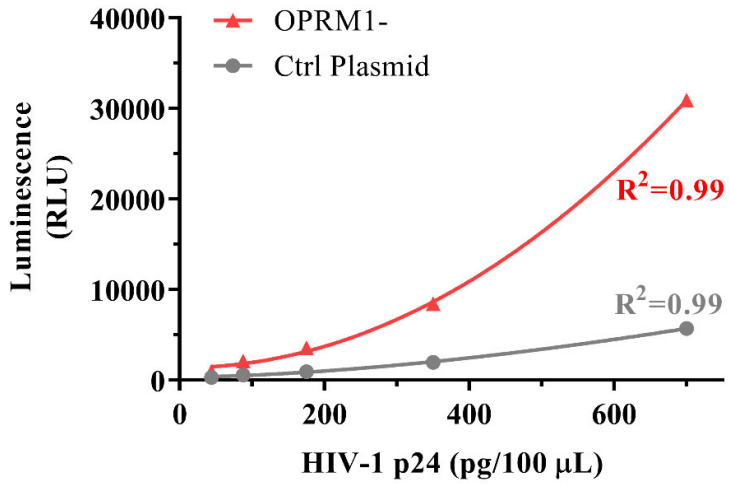

Figure S5. Comparison of intracellular concentration of HIV-1_{BaL} (RLU) in OPRM1- and control plasmid transfected TZM-bl cells.

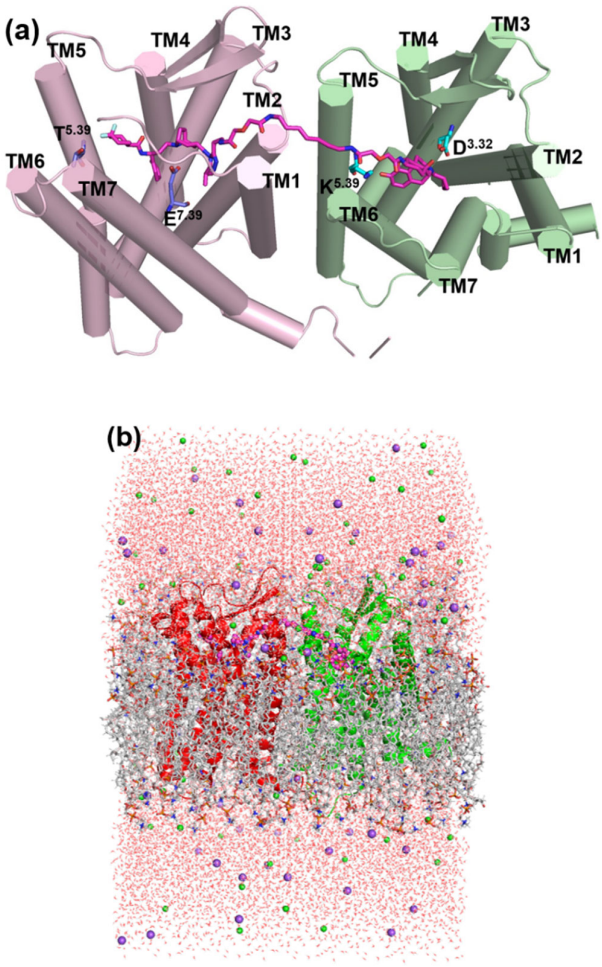

Figure S6. (a) The binding mode of **VZMC013** in the MOR-CCR5 heterodimer complex. (b) The MOR-CCR5_**VZMC013** complex in the membrane-aqueous sodium chloride solution system.

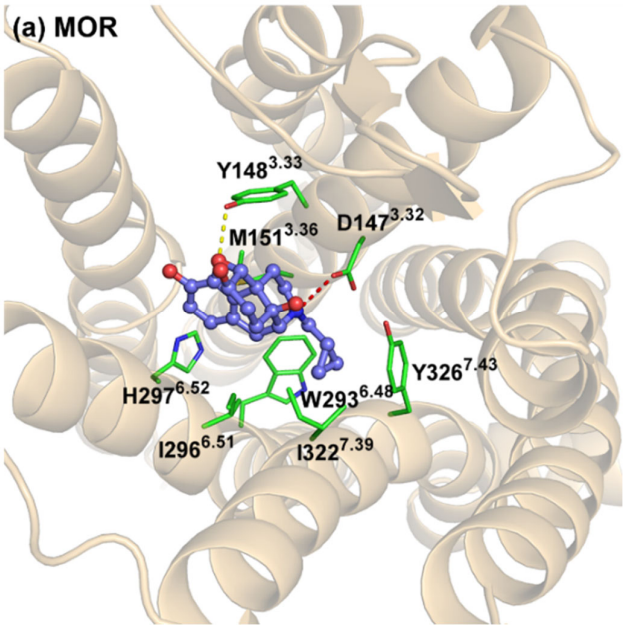
(a) MOR
Y148^3.33
M151^3.36
D147^3.32
H297^6.52
W293^6.48
Y326^7.43
I296^6.51
I322^7.39

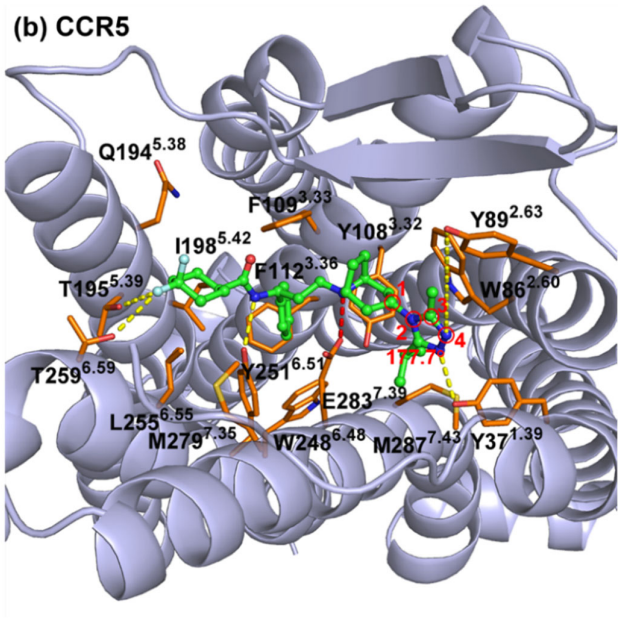
(b) CCR5
Q194^5.38
F109^3.33
Y108^3.32
Y89^2.63
I198^5.42
F112^3.36
T195^5.39
W86^2.60
T259^6.59
Y251^6.51
E283^7.39
L255^6.55
M279^7.35
W248^6.48
M287^7.43
Y37^1.39

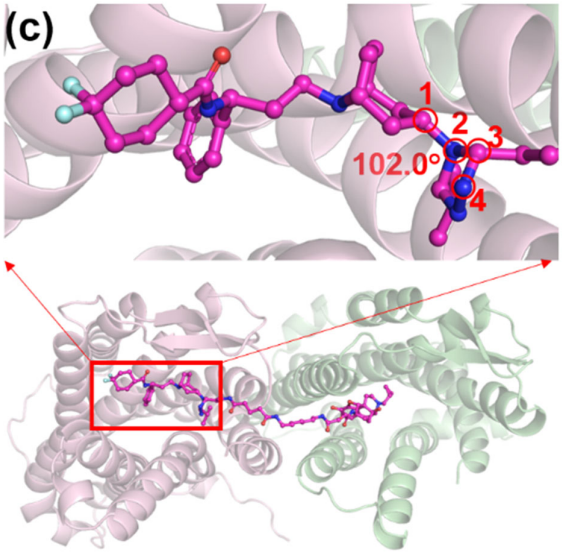

Figure S7. (a) The docking pose of naltrexone in the inactive MOR. (b) The binding mode of maraviroc in the crystal structure of the CCR5. The MOR and CCR5 shown as cartoon models in light-orange and light-blue, respectively. The key residues in the MOR and CCR5 shown as stick models in green and orange, respectively. Naltrexone and maraviroc shown as stick and sphere models in light-blue and green, respectively. The ionic interaction and hydrogen bond shown as dashed lines in red and yellow, respectively. (c) The rotation of the triazole moiety of **VZMC013** in the MOR-CCR5_**VZMC013** complex after 100 ns MD simulation. The atoms related to the dihedral angle were labeled with red circle.

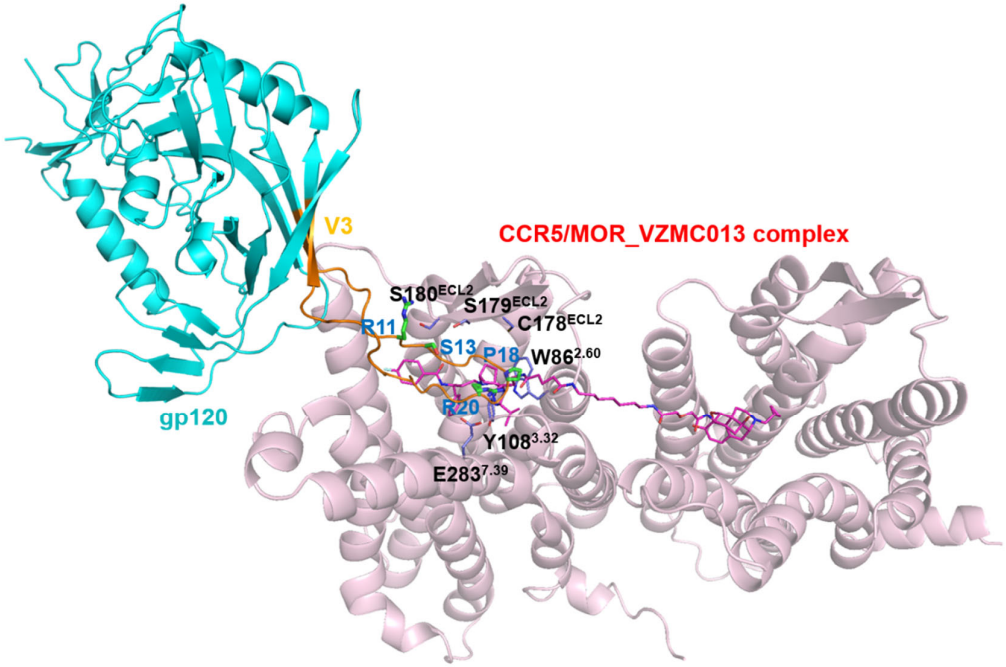

Figure S8. The putative binding of gp120 with the MOR-CCR5_**VZMC013** complex. gp120 shown as a cartoon model in cyan. V3 loop of gp120 shown as a cartoon model in orange. MOR-CCR5 heterodimer shown as a cartoon model in pink. Compound **VZMC013** shown as a stick model in magentas. Key residues of the CCR5 and V3 loop shown as stick models in light-blue and green, which labeled in black and blue text, respectively.

Table S1. MOR radioligand binding affinity.

Compounds	Ki (nM)
VZMC002	9.2 ± 3.4[a]
Naltrexone	0.7 ± 0.1[a]

[a]Data have been reported in Reference 1, and are presented here for comparison.

Table S2. CCR5 radioligand binding affinity.[a]

Compounds	Ki (nM)[b]
VZMC014	41 ± 1
VZMC018	7.15 ± 0.26
VZMC020	ND[c]
MIP-1β	0.056 ± 0.006

[a][^{125}I]MIP-1α was used as the radioligand in the binding assay.

[b]Ki values were calculated using the Cheng-Prusoff equation. The values are the mean ± SEM of at least three independent experiments.

[c]Not determined.

Table S3. Inhibition of CCL5-stimulated intracellular Ca^{2+} mobilization.[a]

Compounds	IC_{50} (nM)
VZMC014	116 ± 2.53
VZMC018	39.6 ± 4.01
VZMC020	919 ± 45.4
VZMC003	622 ± 36[b]
Maraviroc	0.77 ± 0.20

[a]The values are the mean ± SEM of at least three independent experiments.

[b]Data have been reported in Reference 1, and are presented here for comparison purposes.

Table S4. Inhibition of HIV-1_{BaL} and cytotoxicity in GHOST CCR5 cells.[a]

Compounds	EC_{50} (μM)	TC_{50} (μM)	TI
VZMC014	2.62 ± 1.25	> 100	> 38
VZMC002	> 100	> 100	-
Maraviroc	0.018 ± 0.002	> 0.5	> 28

[a] Measured in triplicate.

Table S5. Residues within 5 Å proximity of the bivalent ligand in association with the MOR-CCR5_**VZMC013** complex after 100 ns MD simulations.[a]

Portions of the bivalent ligand **VZMC013**	Interactional residues
The CCR5 pharmacophore	**Y37$^{1.39}$**, **W86$^{2.60}$**, **Y89$^{2.63}$**, **Y108$^{3.32}$**, **F109$^{3.33}$**, **F112$^{3.36}$**, N163$^{4.64}$, C178^{ECL2}, S179^{ECL2}, S180^{ECL2}, F182^{ECL2}, **T195$^{5.39}$**, **I198$^{5.42}$**, **W248$^{6.48}$**, **Y251$^{6.51}$**, **L255$^{6.55}$**, **T259$^{6.59}$**, **E283$^{7.39}$**, **M287$^{7.43}$**
The MOR pharmacophore	**D147$^{3.32}$**, **Y148$^{3.33}$**, **M151$^{3.36}$**, L232$^{5.38}$, V236$^{5.42}$, **I296$^{6.51}$**, **H297$^{6.52}$**, V300$^{6.55}$, W318$^{7.35}$, **I322$^{7.39}$**
Spacer	A30$^{1.32}$, R31$^{1.33}$, A87$^{2.61}$, A90$^{2.64}$, A91$^{2.65}$, W226$^{5.32}$, N230$^{5.36}$, E229$^{5.35}$, K233$^{5.39}$, K303$^{6.58}$

[a]The residues in **Bold** represented the residues playing important roles in the binding of compound **VZMC013** with the MOR-CCR5 heterodimer and these residues also presented in the binding of maraviroc and naltrexone in their respective receptors, the CCR5 and MOR.

Table S6. Residues with 5 Å around maraviroc and naltrexone in the respective receptors, CCR5 and MOR.[a]

Complex	Residues
CCR5_ Maraviroc	**Y37$^{1.39}$**, **W86$^{2.60}$**, **Y89$^{2.63}$**, **Y108$^{3.32}$**, **F109$^{3.33}$**, **F112$^{3.36}$**, Q194$^{5.38}$, **T195$^{5.39}$**, **I198$^{5.42}$**, **W248$^{6.48}$**, **Y251$^{6.51}$**, **L255$^{6.55}$**, **T259$^{6.59}$**, M279$^{7.35}$, **E283$^{7.39}$**, **M287$^{7.43}$**
MOR_Naltrexone	**D147$^{3.32}$**, **Y148$^{3.33}$**, **M151$^{3.36}$**, W293$^{6.48}$, **I296$^{6.51}$**, **H297$^{6.52}$**, **I322$^{7.39}$**, **Y326$^{7.43}$**

[a]The residues in **Bold** represented the residues played important roles in the binding of maraviroc and naltrexone with their respective receptors, CCR5 and MOR, also existed in the binding of compound **VZMC013** with the MOR-CCR5 heterodimer.

Table S7. The distances between atom of ligand and atom of receptor in the MOR_naltrexone, CCR5_maraviroc, and MOR-CCR5_**VZMC013** complexes.

Complex	Atom@Ligand	Atom@Receptor	Distance (Å)
MOR_naltrexone	N17	OD2@D147$^{3.32}$	3.0
	O15	OH@Y148$^{3.33}$	2.8
	C5	CZ3@W293$^{6.48}$	4.6
	C36	CZ@Y326$^{7.43}$	3.6
CCR5_maraviroc	C9	CB@C178^{ECL2}	8.1
	C22	CZ@F182^{ECL2}	5.4
	O1	OG@S179^{ECL2}	6.0
	O1	OG@S180^{ECL2}	5.8
MOR-CCR5_**VZMC013**	N17	OD2@D147$^{3.32}$	7.1
	O15	OH@Y148$^{3.33}$	6.4
	C5	CZ3@W293$^{6.48}$	8.2
	C36	CZ@Y326$^{7.43}$	7.3
	C9	CB@C178^{ECL2}	5.2
	C22	CZ@F182^{ECL2}	3.5
	O1	OG@S179^{ECL2}	3.4
	O1	OG@S180^{ECL2}	3.6

Spectra of key intermediate 24 and target compounds

^{1}H NMR, ^{13}C NMR, ^{19}F NMR, and HRMS spectra for **24**

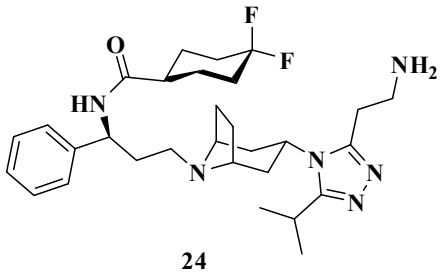

24

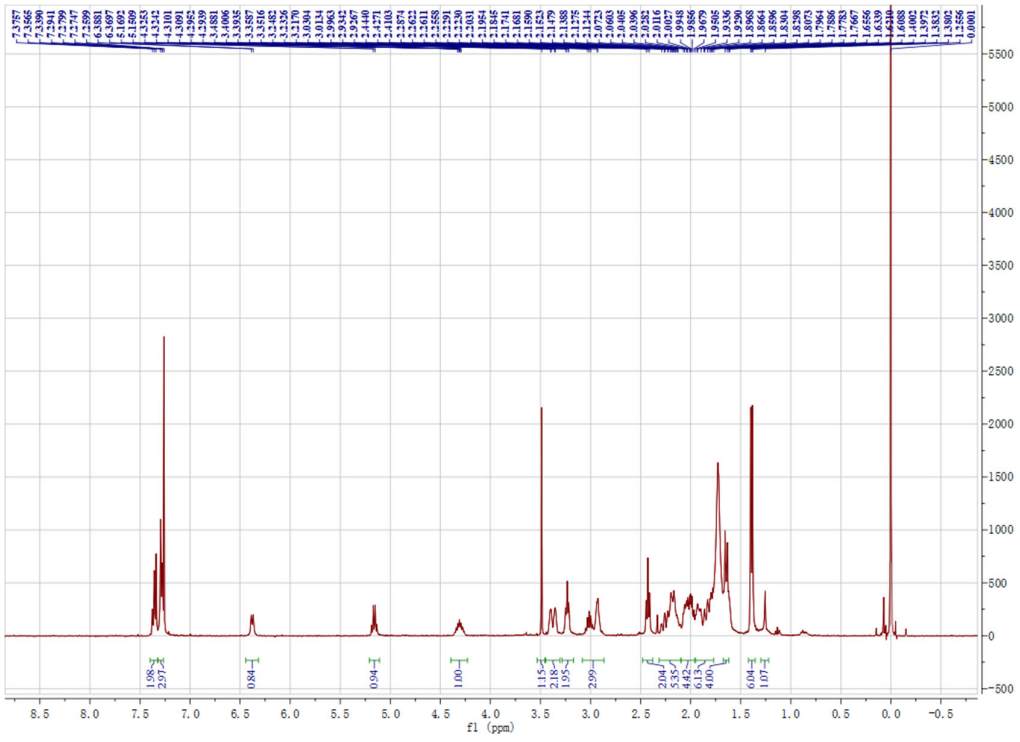

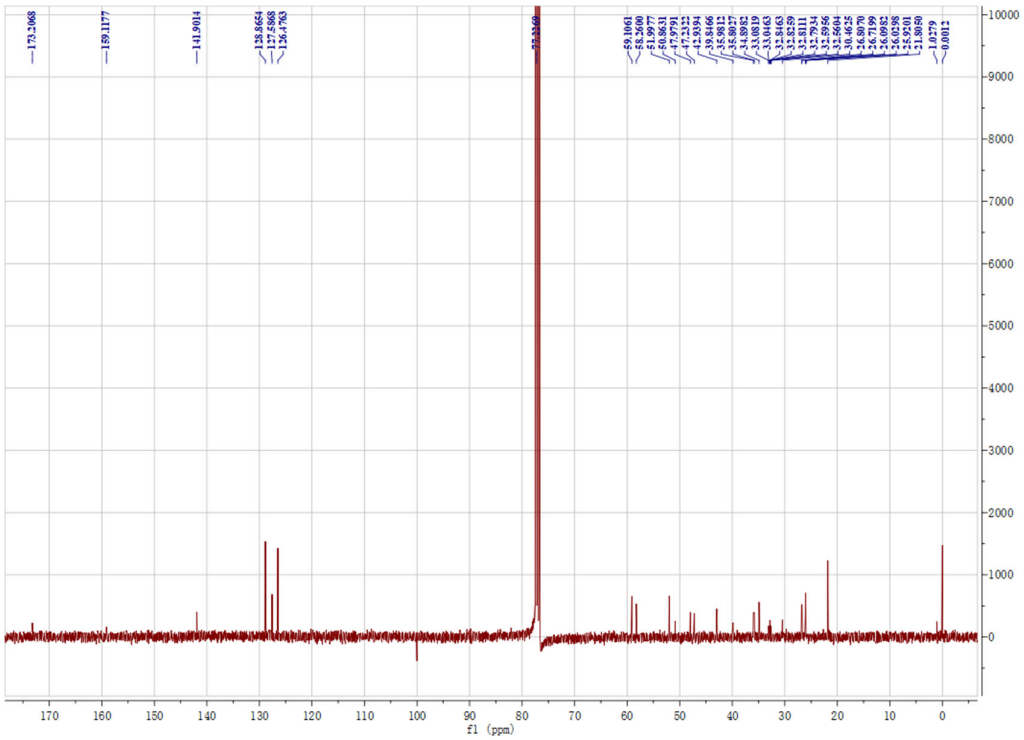
173.2068
169.1177
141.9014
136.8664
127.5868
126.9765
77.3160
59.1061
58.2600
51.9977
50.9631
47.9791
47.2322
42.9394
39.8466
35.8812
34.8857
33.0463
33.0619
32.8463
32.8259
32.7911
32.7834
32.5956
32.5604
30.4625
26.8070
25.7199
25.6985
25.6298
25.5201
21.8050
1.0279
0.0012
f1 (ppm)

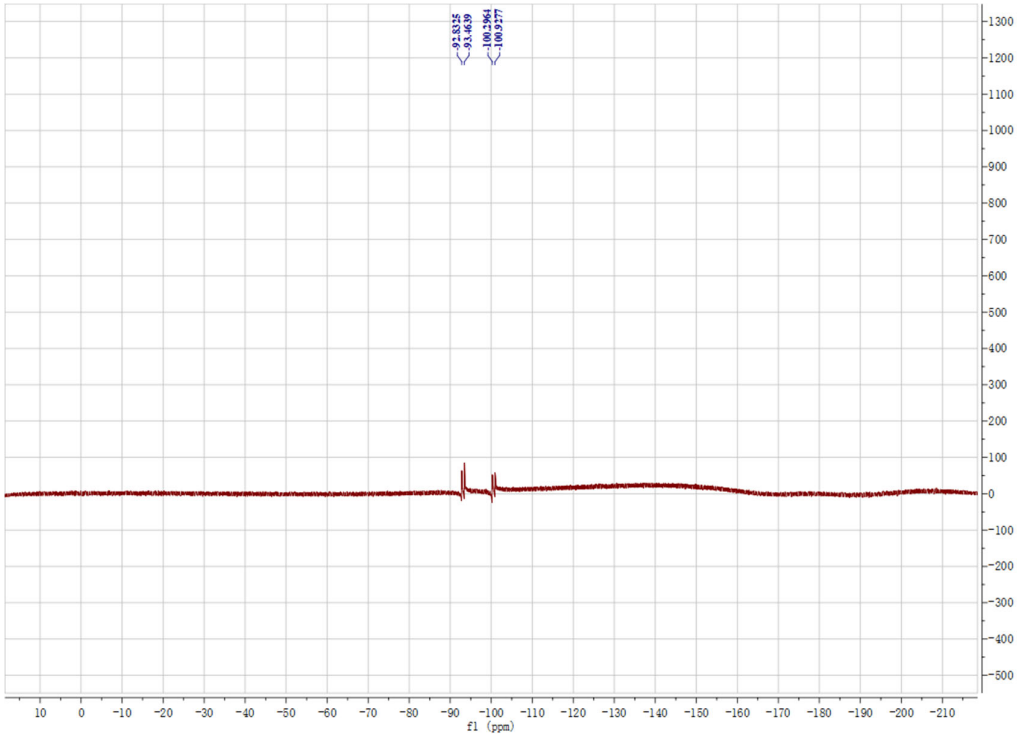
93.8325
93.4639
100.2964
100.9277
f1 (ppm)

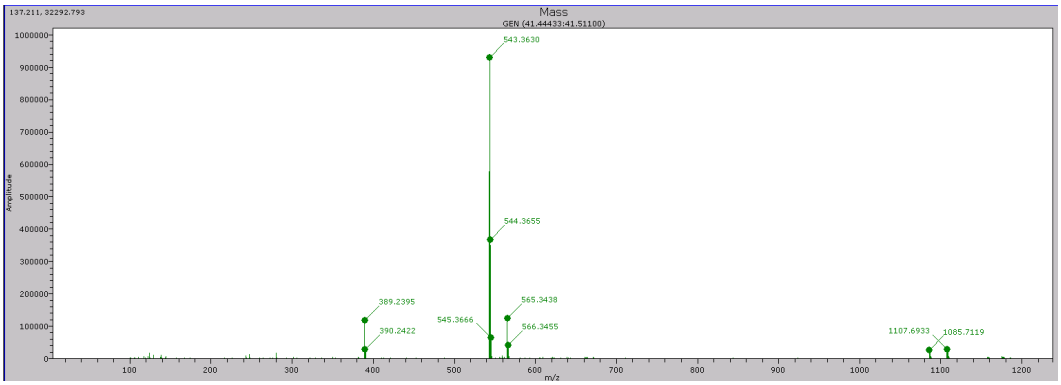

^{1}H NMR, ^{13}C NMR, ^{19}F NMR, and HRMS spectra for **VZMC013**

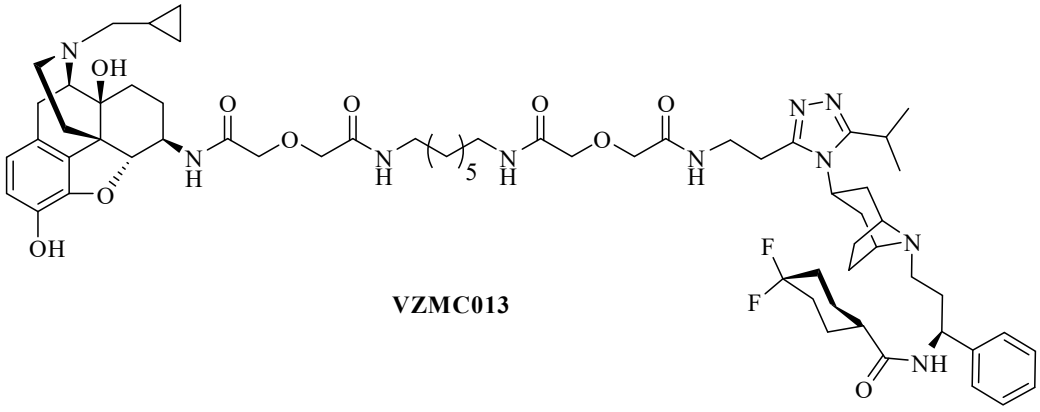

VZMC013

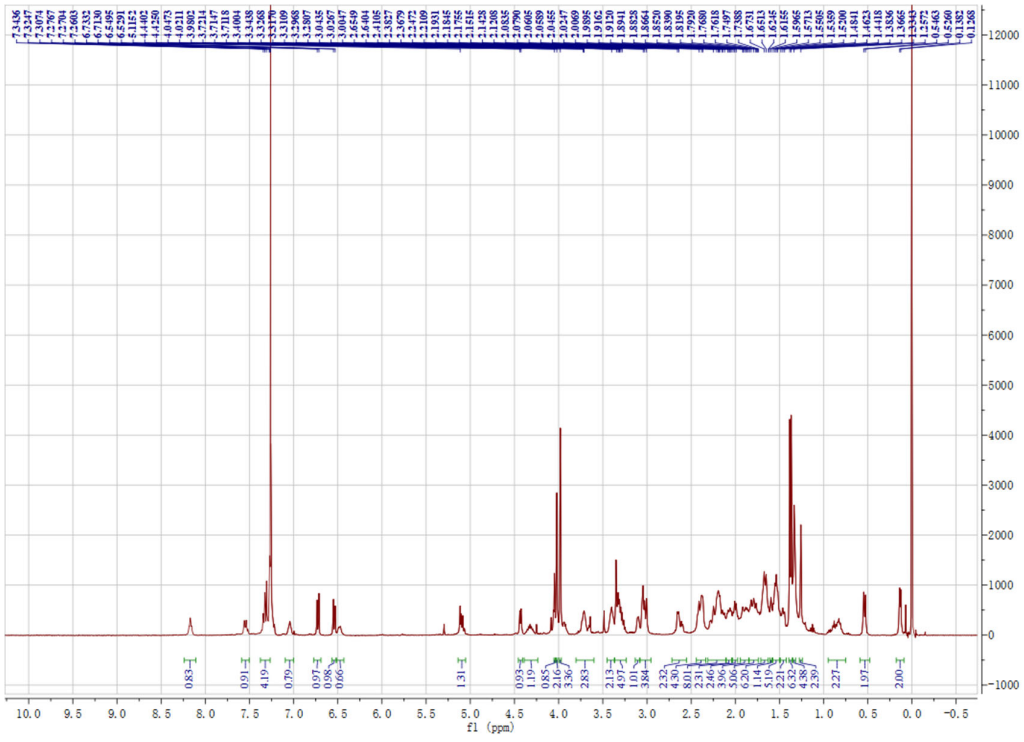

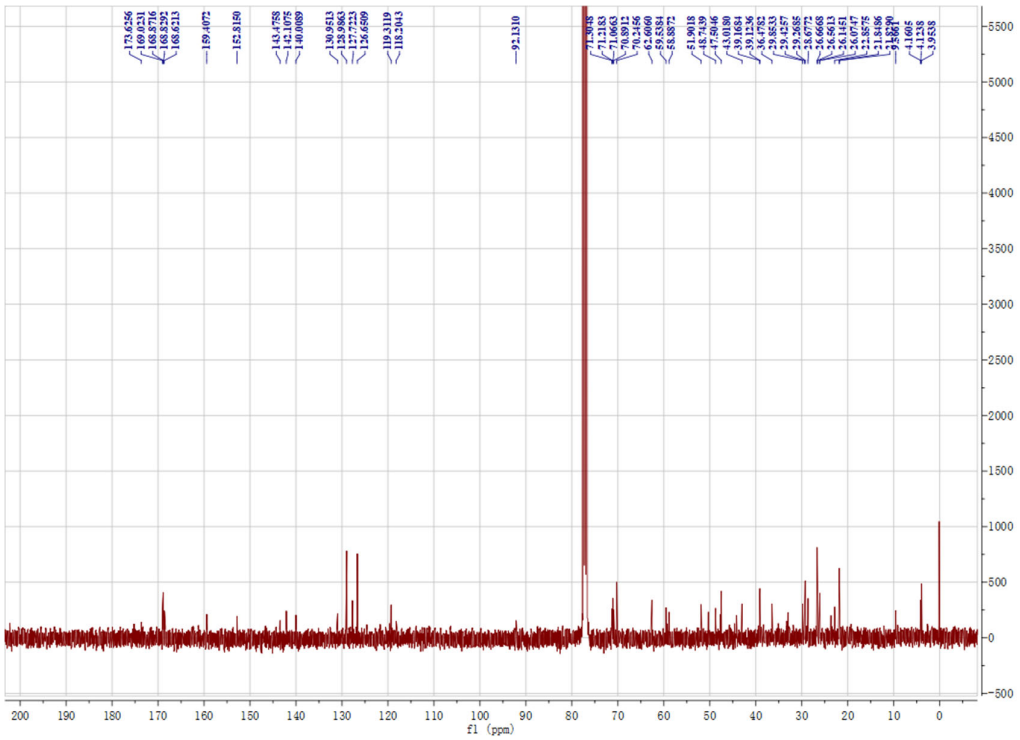
173.6256
169.0231
168.8716
168.8292
168.6213
159.4072
152.8150
143.4758
142.1075
140.0089
130.9513
128.9863
125.7223
126.6509
119.3119
118.2043
92.1310
71.2648
71.2183
71.0663
70.8911
70.2456
67.6660
65.8584
65.8872
51.9018
51.7619
47.7939
47.7646
43.0180
39.1684
39.1256
38.6782
38.4753
29.4257
29.2685
28.6772
26.6668
26.6613
26.1455
26.0747
25.8575
21.8486
21.8270
14.1605
14.1238
3.9538
f1 (ppm)

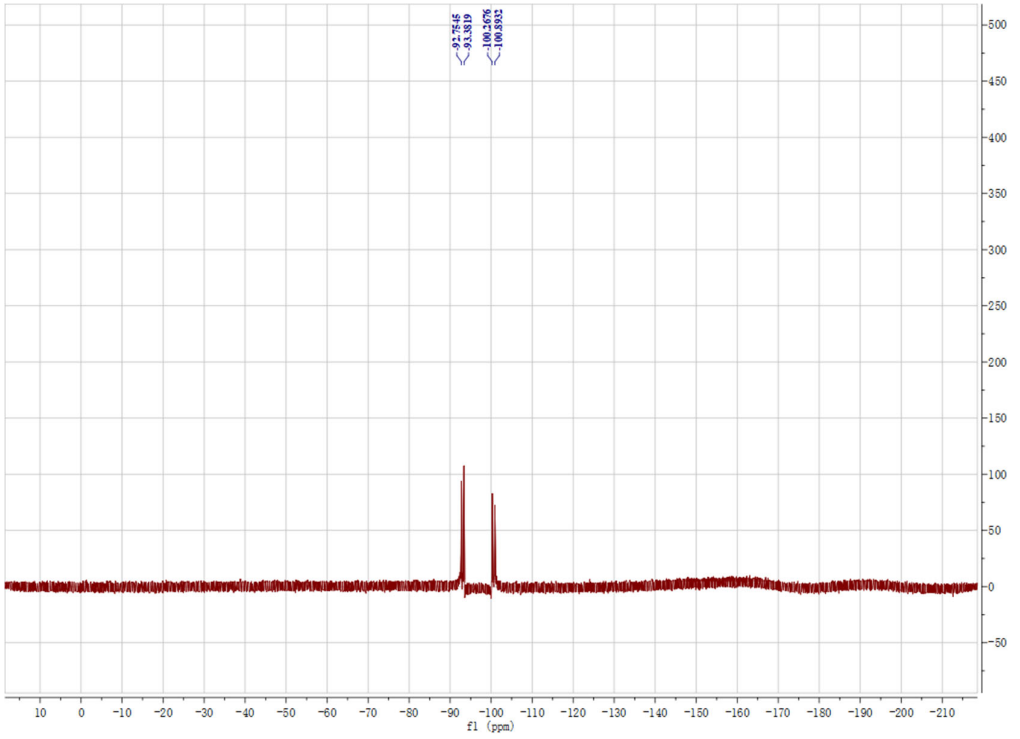
93.7545
93.3819
100.2676
100.8932
f1 (ppm)

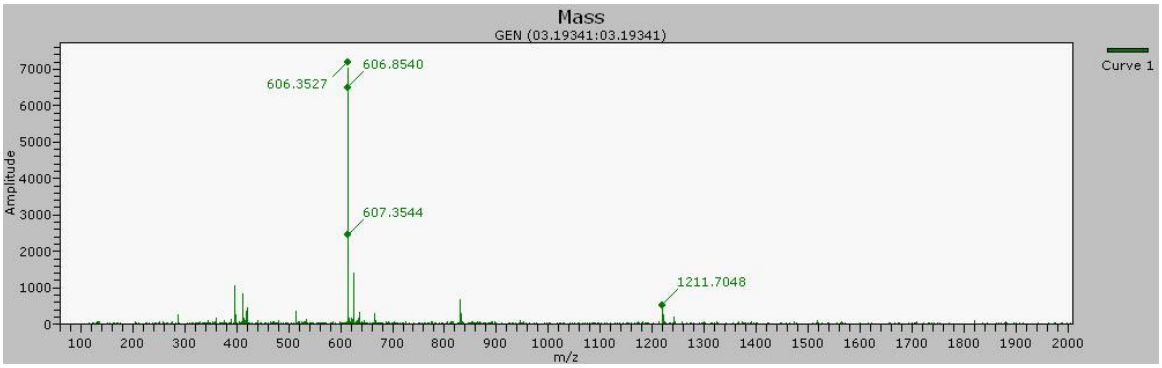

^{1}H NMR, ^{13}C NMR, ^{19}F NMR, and HRMS spectra for **VZMC014**

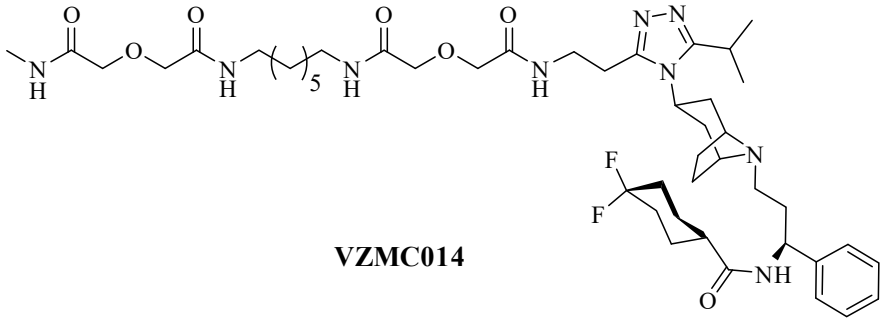

VZMC014

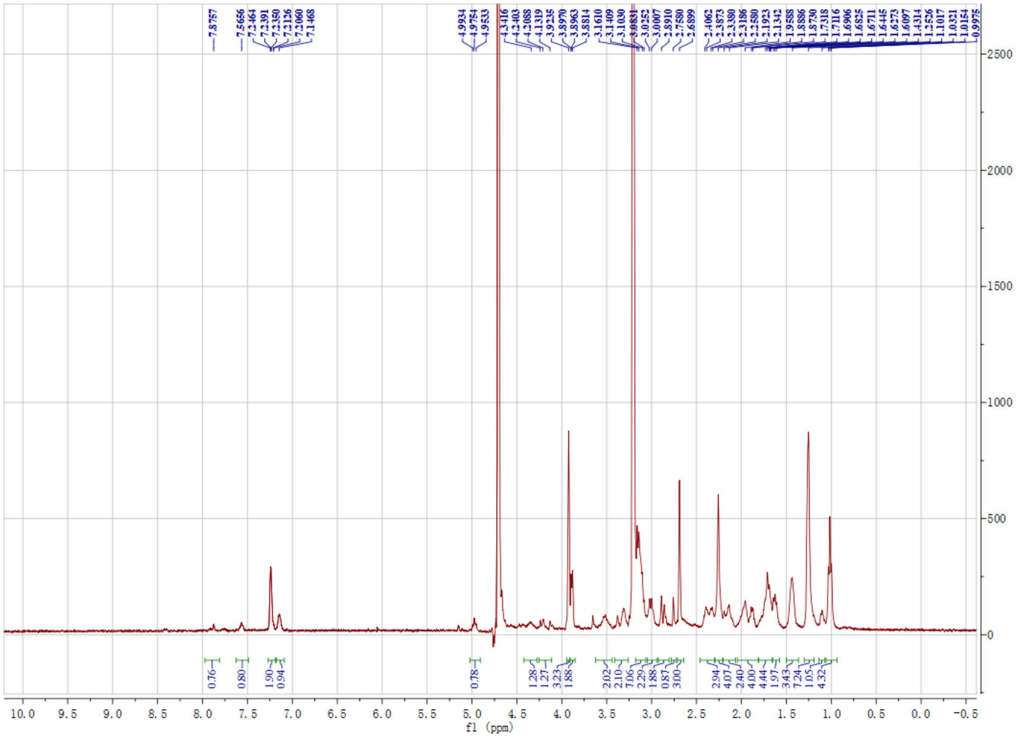

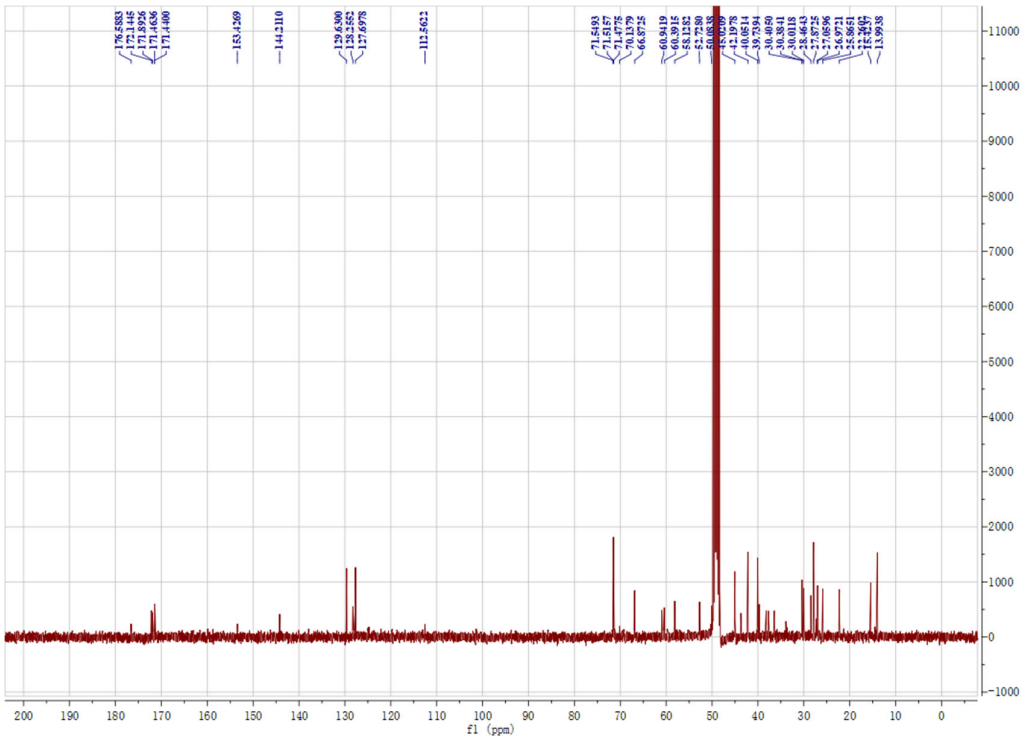
f1 (ppm)

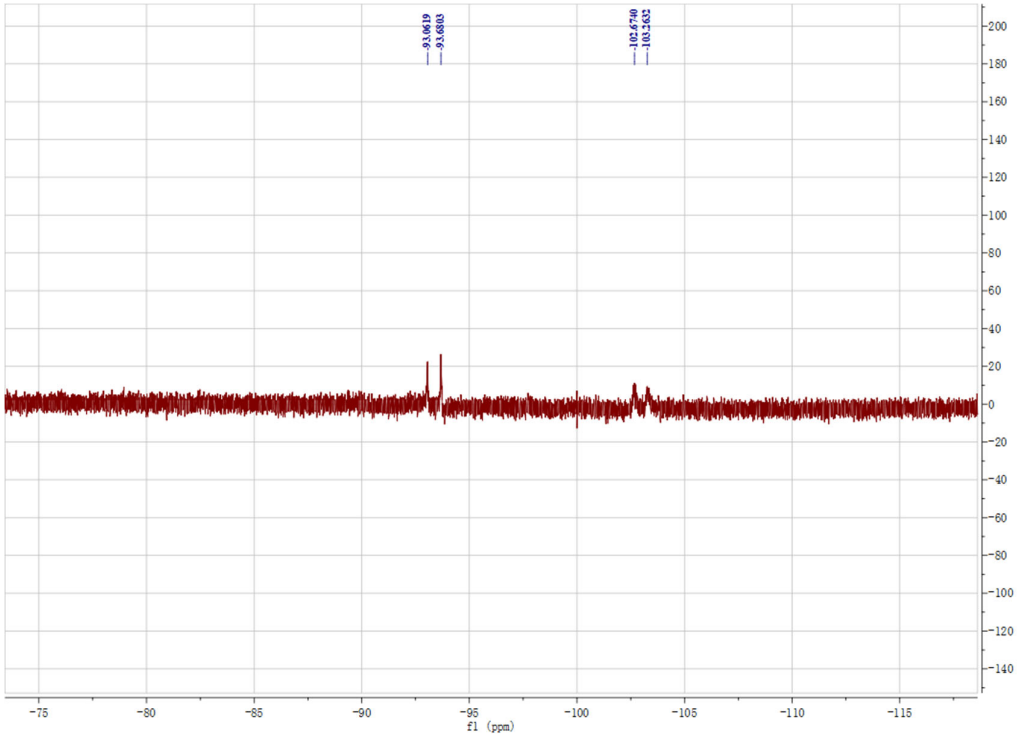
f1 (ppm)

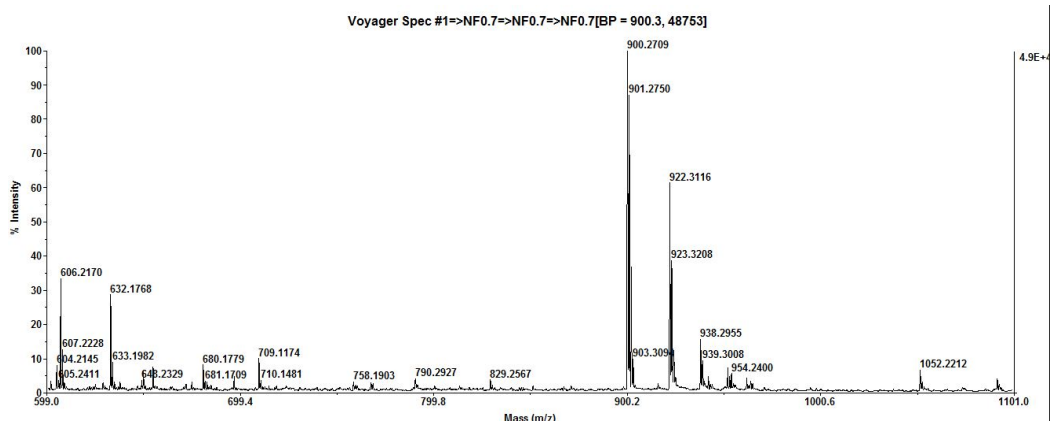

^{1}H NMR, ^{13}C NMR, ^{19}F NMR, and HRMS spectra for **VZMC017**

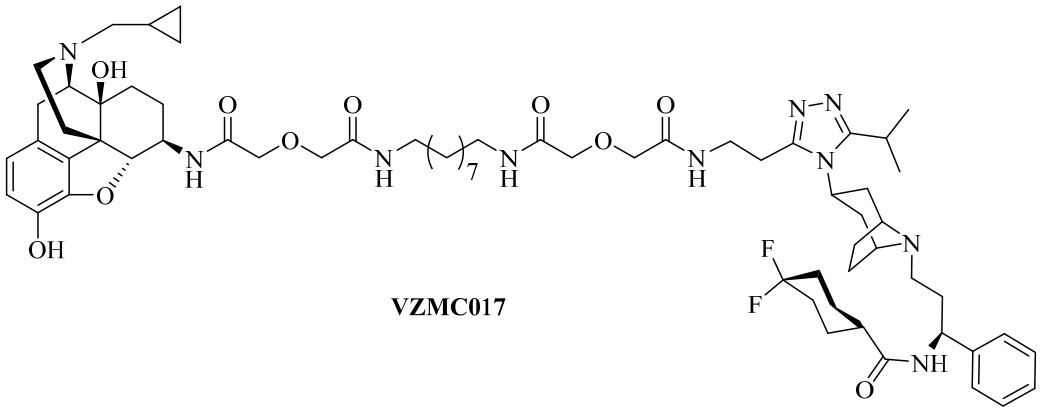

VZMC017

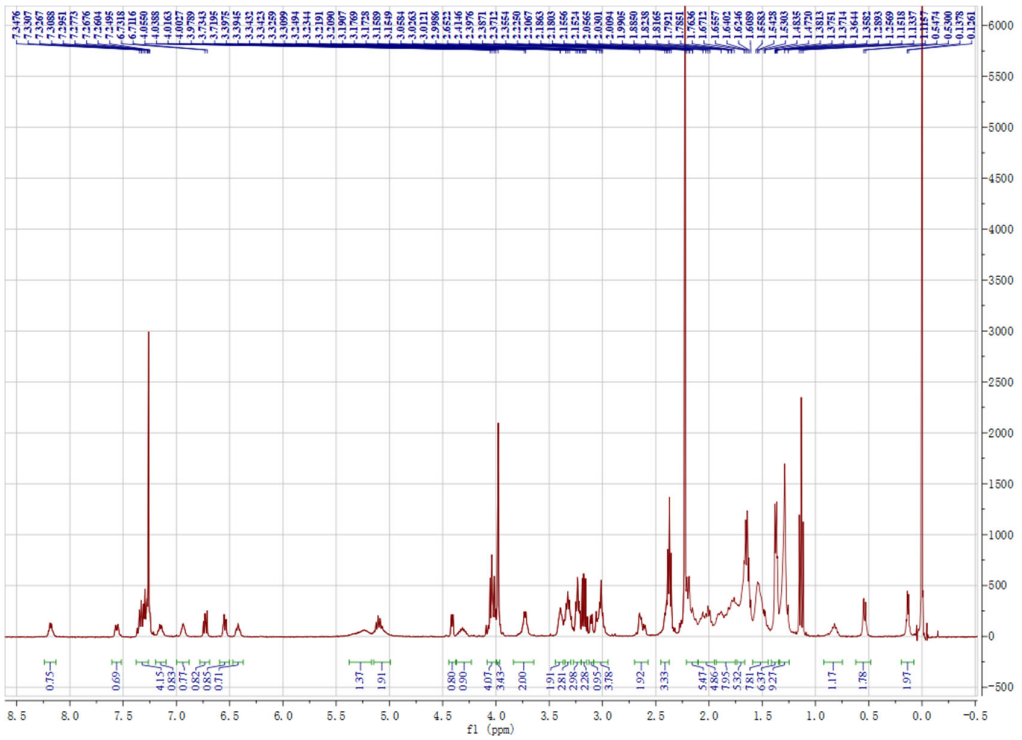
f1 (ppm)

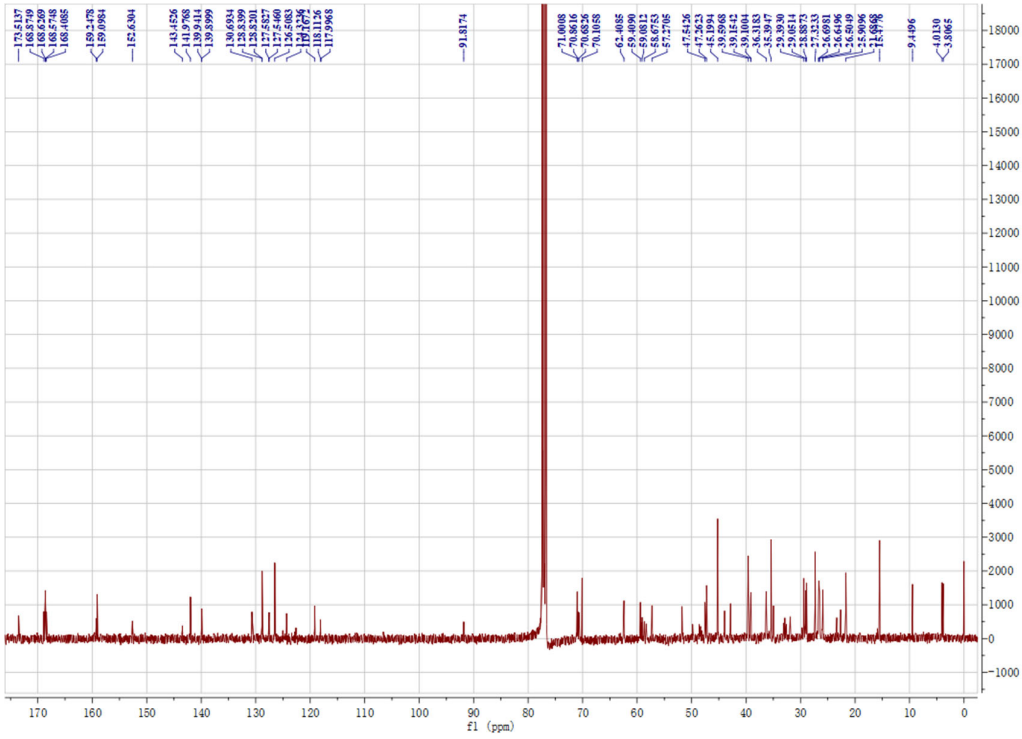
f1 (ppm)

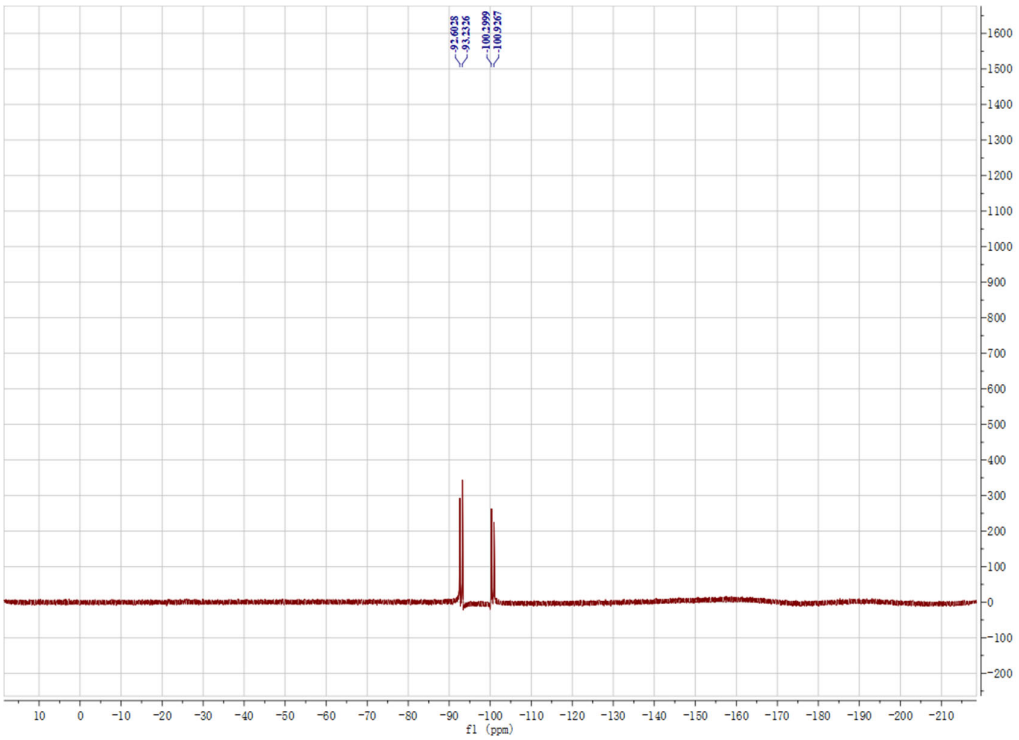

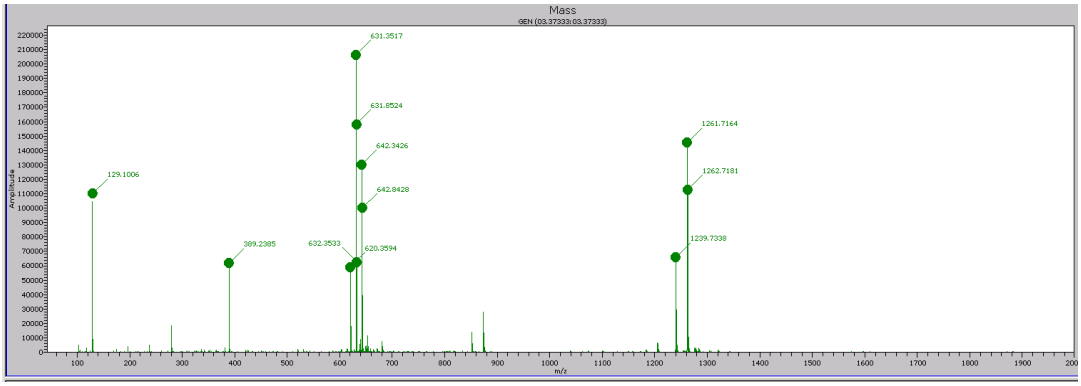

^{1}H NMR, ^{13}C NMR, ^{19}F NMR, and HRMS spectra for **VZMC018**

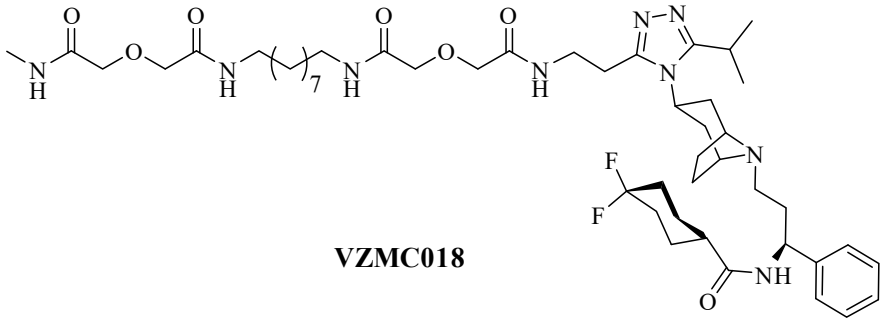

VZMC018

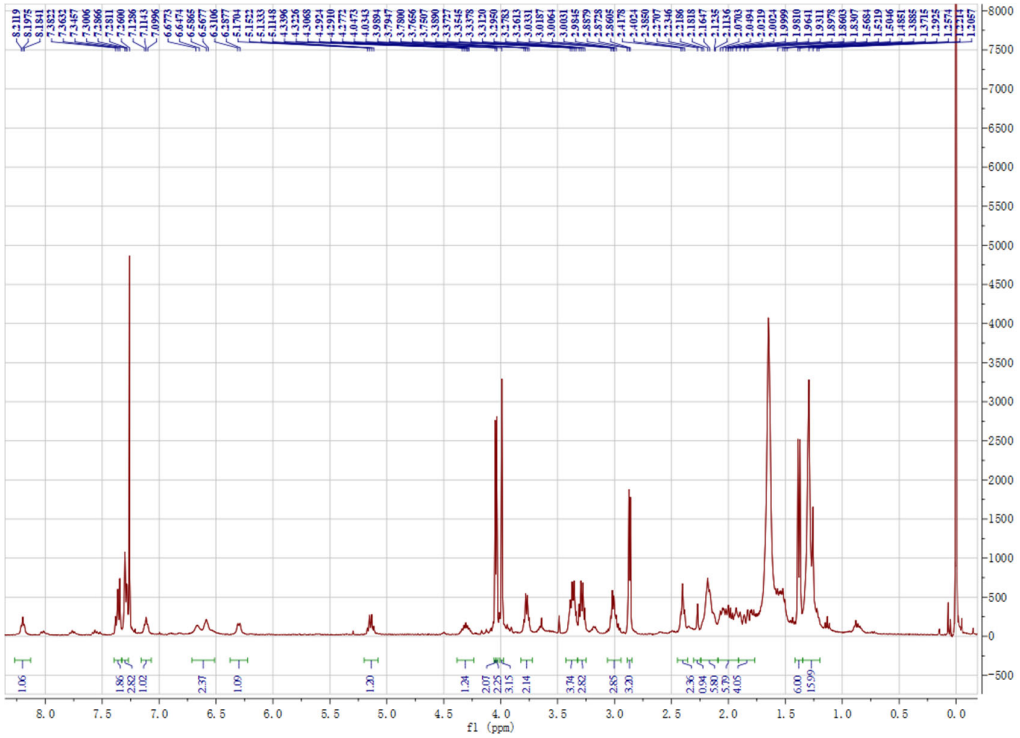
f1 (ppm)

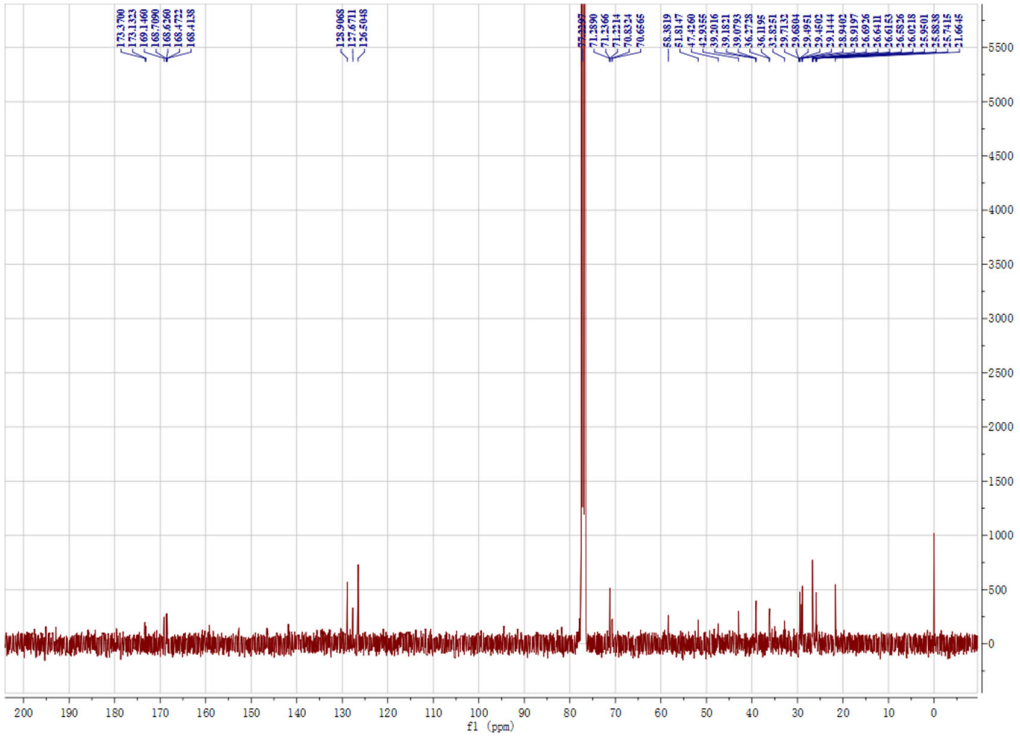
f1 (ppm)

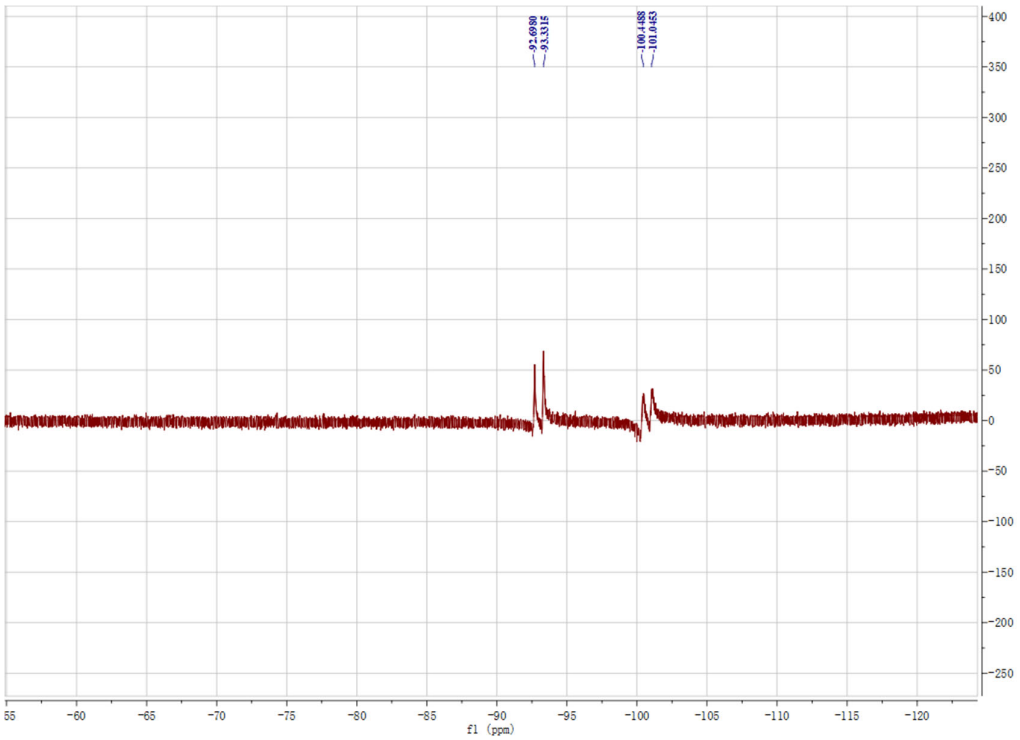

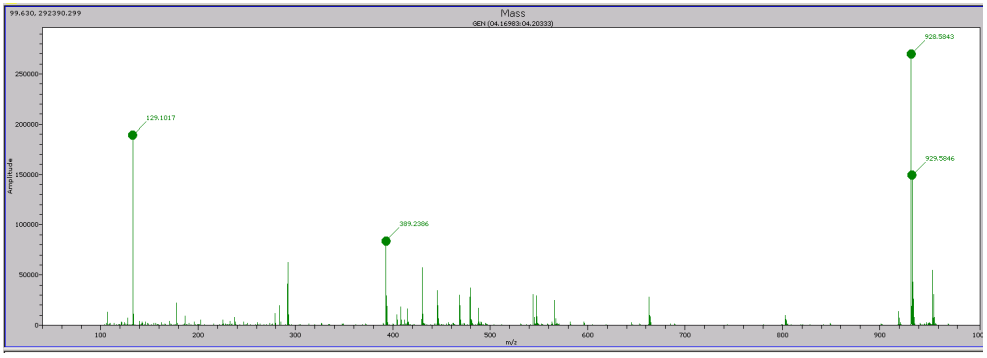

^{1}H NMR, ^{13}C NMR, ^{19}F NMR, and HRMS spectra for **VZMC019**

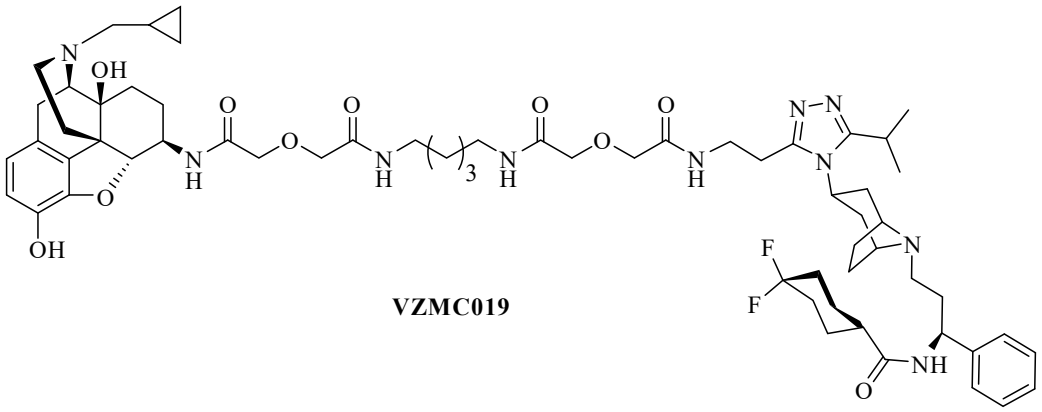

VZMC019

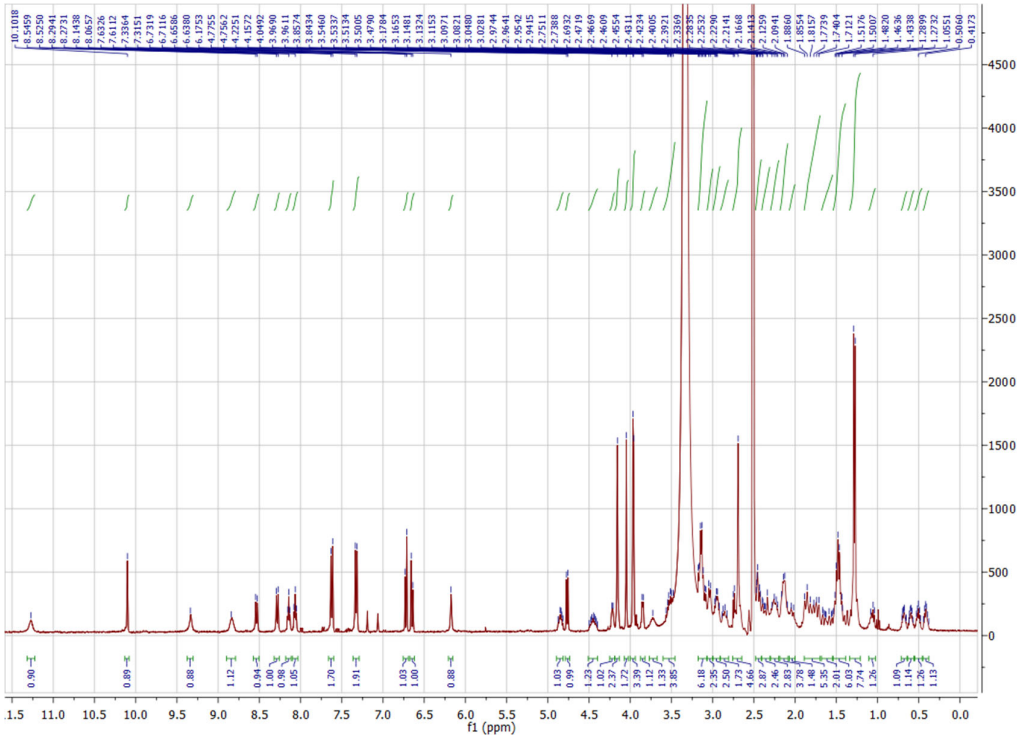
f1 (ppm)

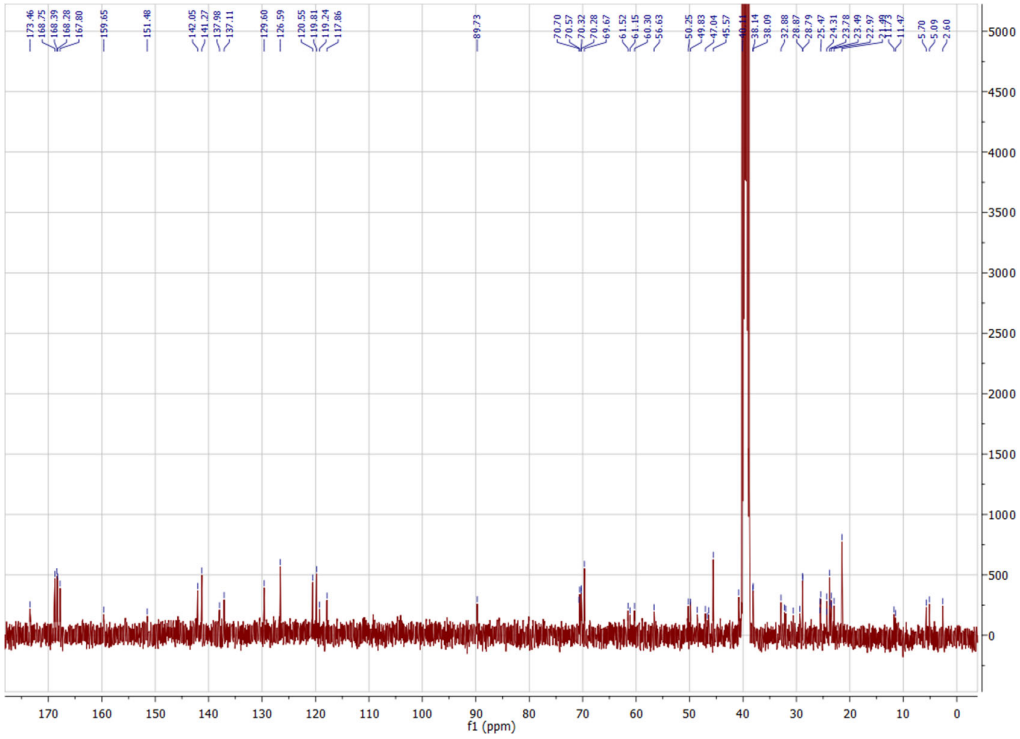
f1 (ppm)

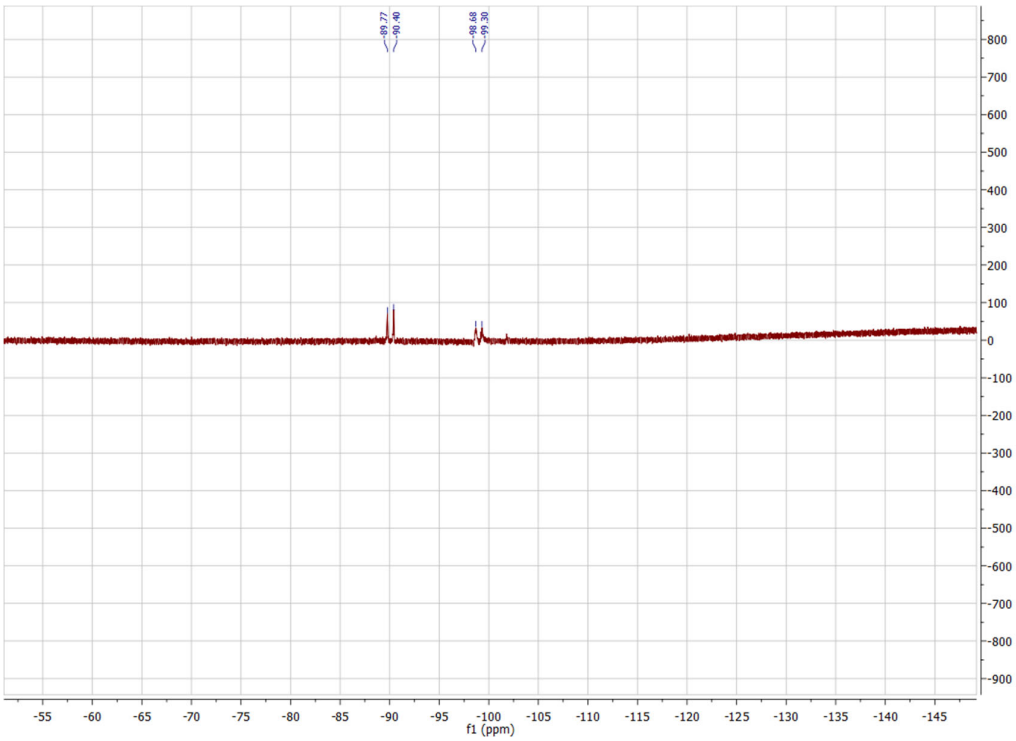

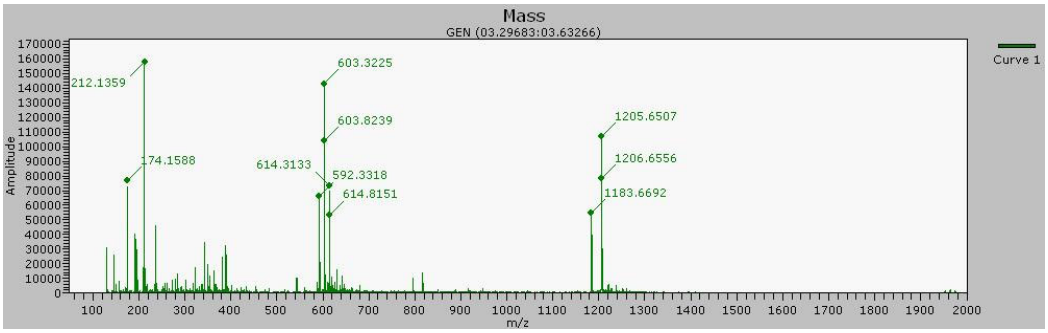

^{1}H NMR, ^{13}C NMR, and ^{19}F NMR spectra for **VZMC020**

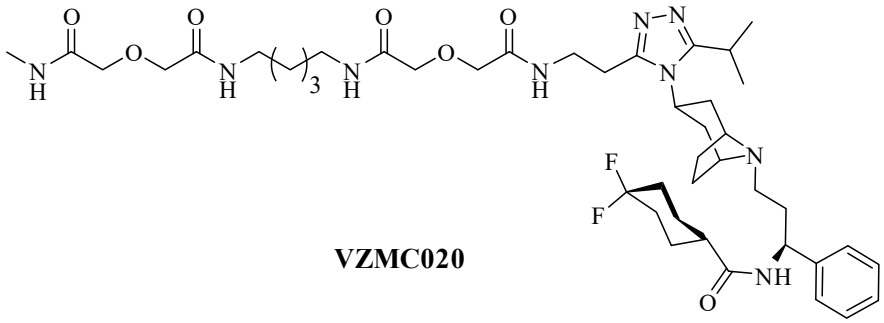

VZMC020

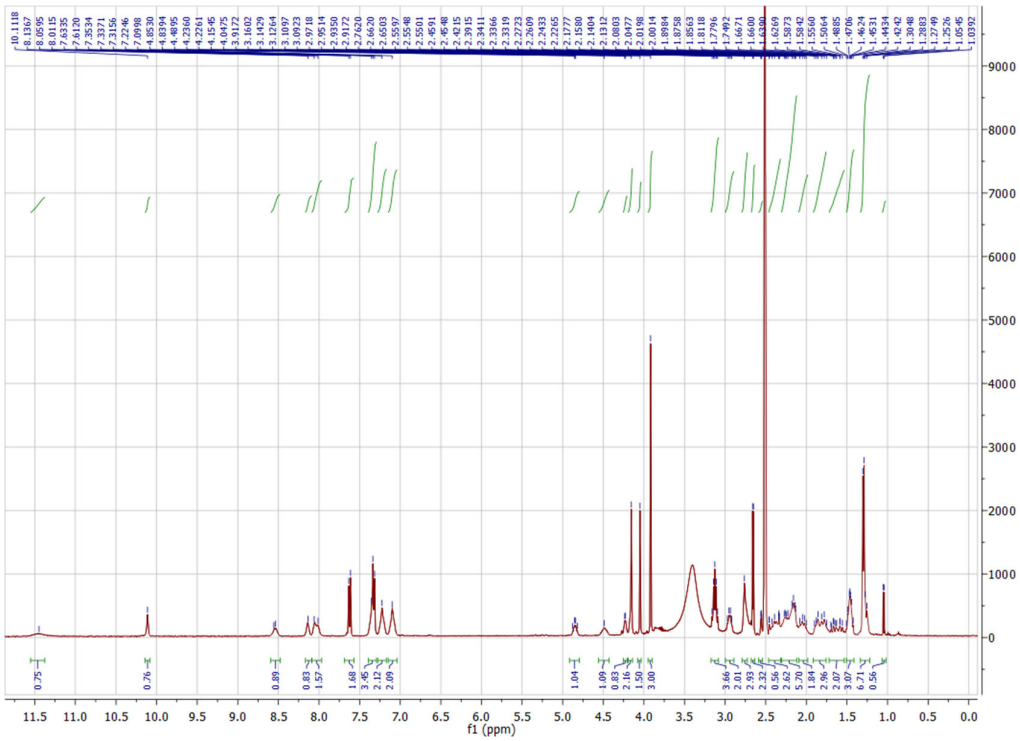
f1 (ppm)

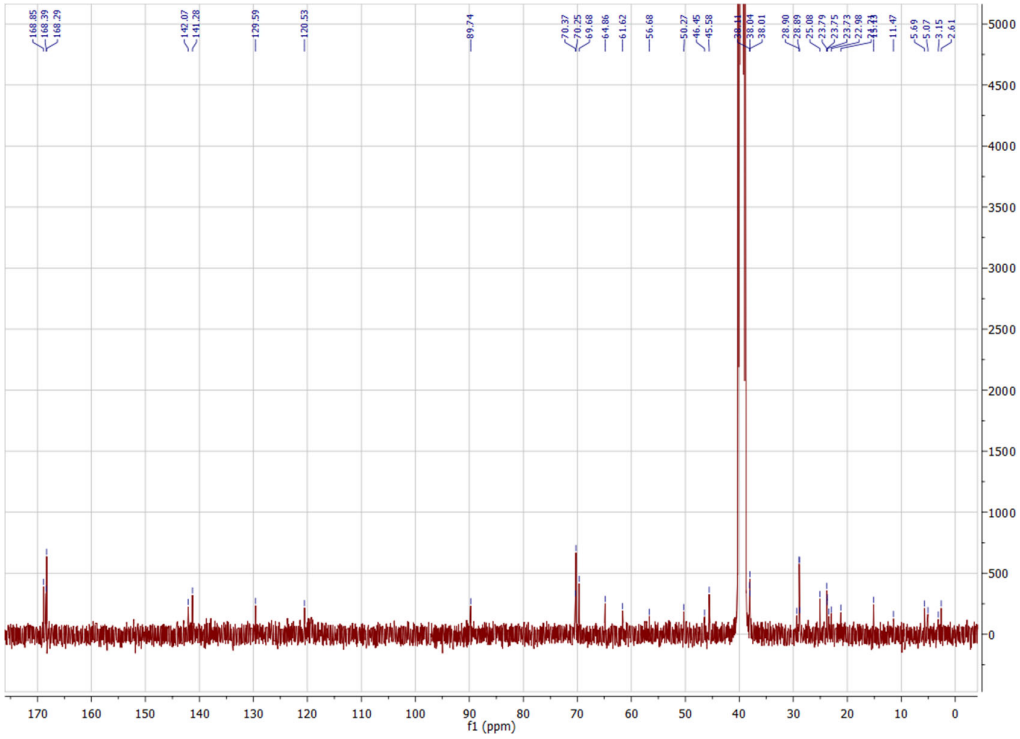
f1 (ppm)

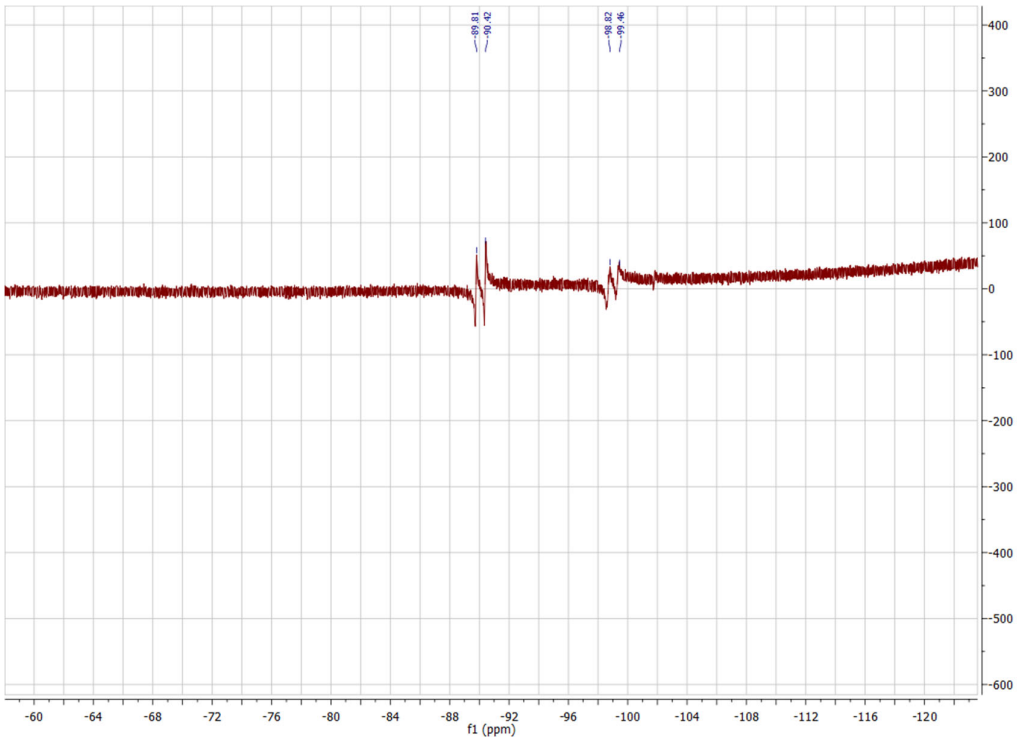

HPLC analysis

VZMC013

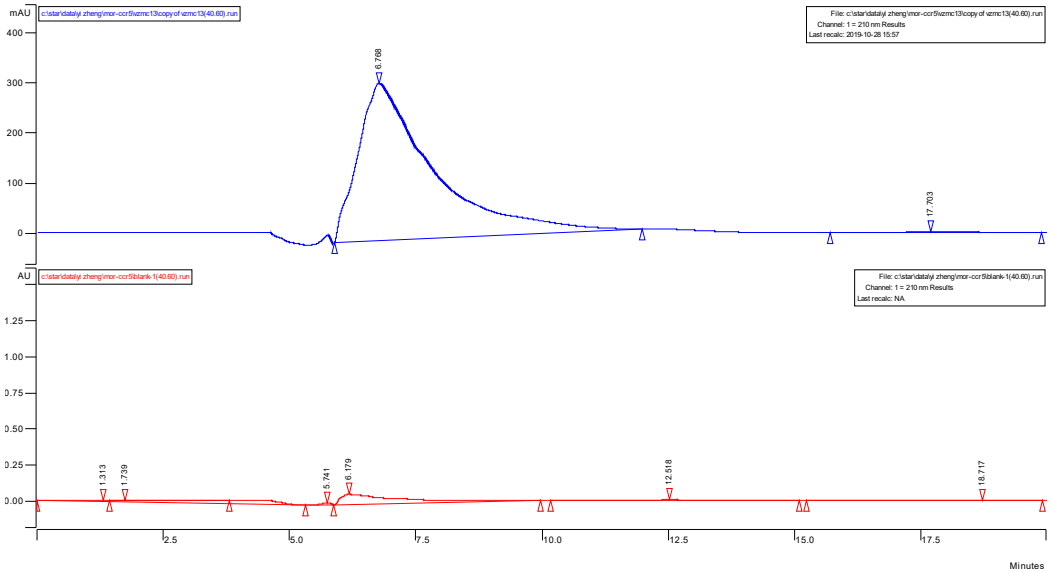

VZMC014

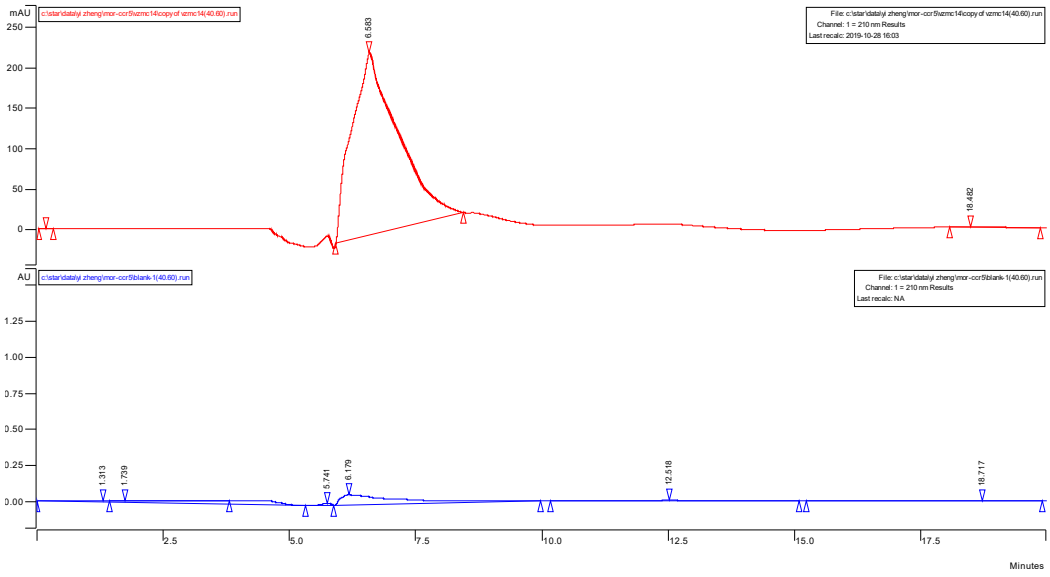

VZMC017

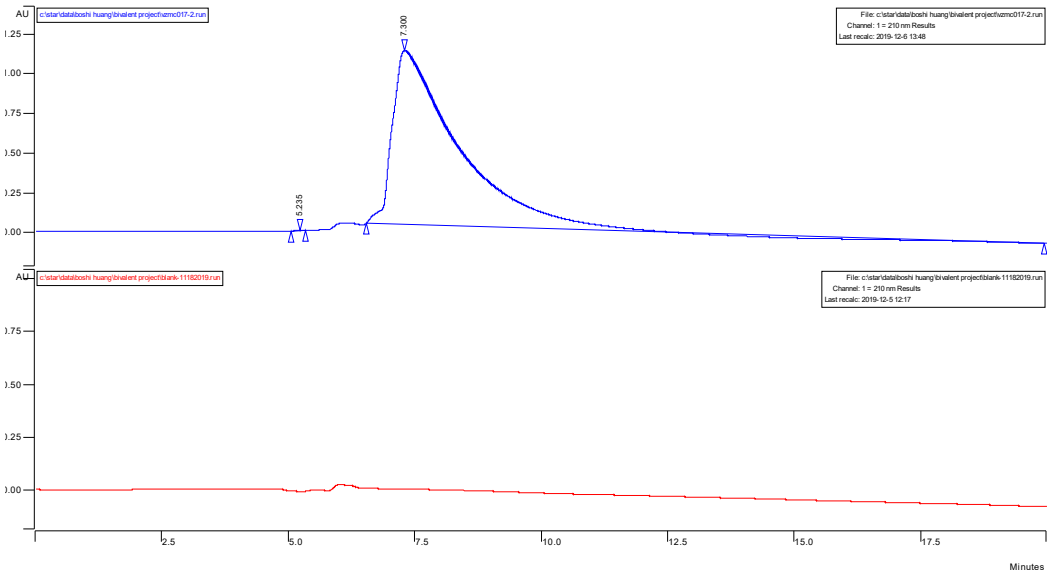

VZMC018

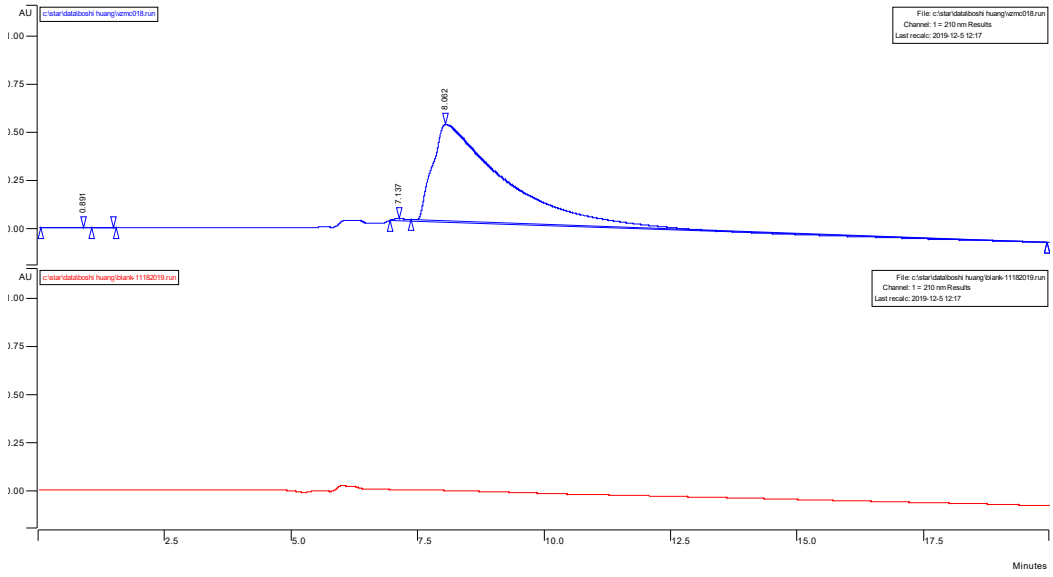

VZMC019

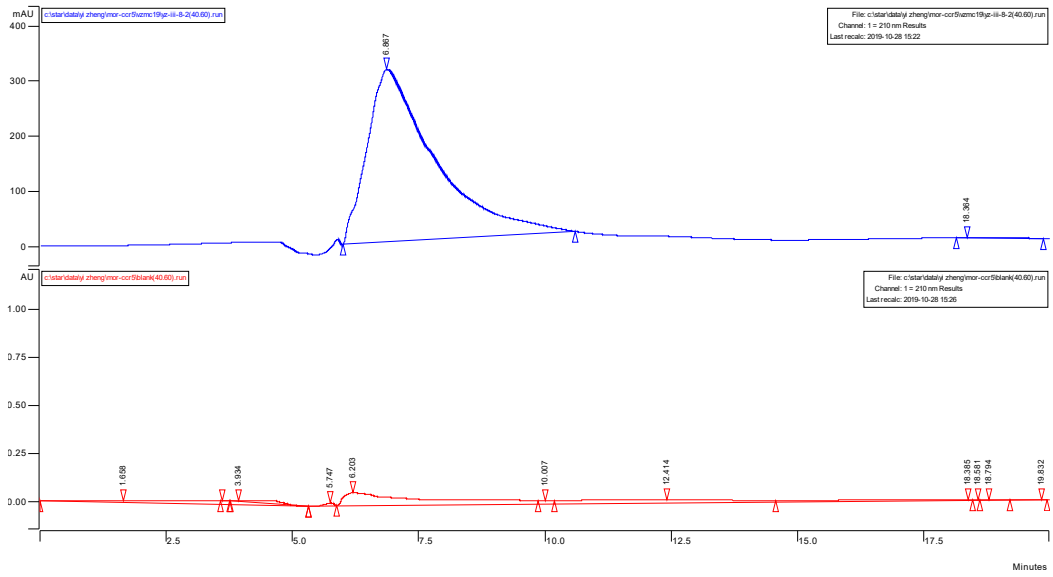

VZMC020

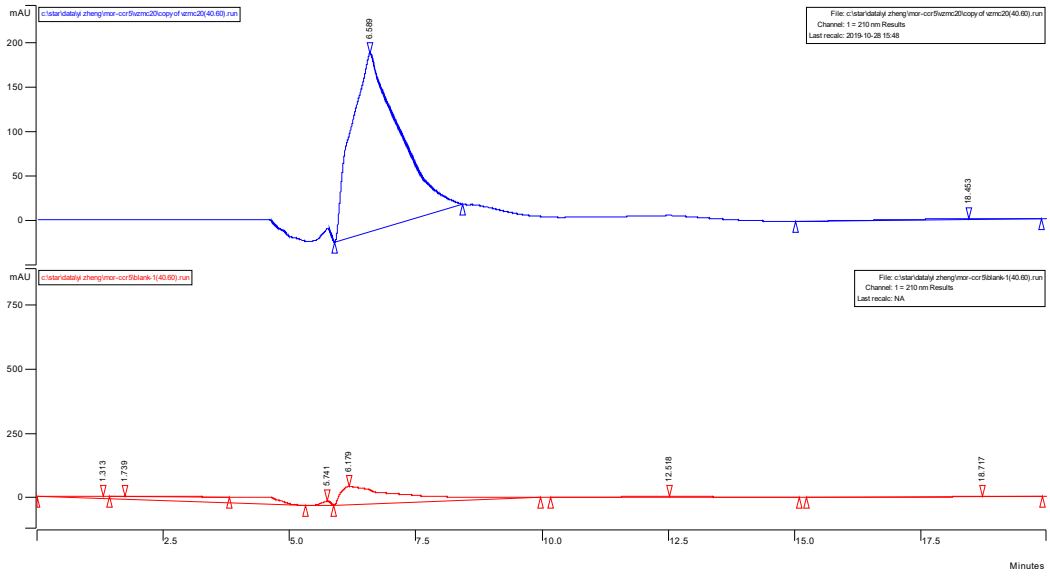

References

1. Yuan, Y.; Arnatt, C. K.; El-Hage, N.; Dever, S. M.; Jacob, J. C.; Selley, D. E.; Hauser, K. F.; Zhang, Y., A bivalent ligand targeting the putative mu opioid receptor and chemokine receptor CCR5 heterodimer: binding affinity versus functional activities. *MedChemComm* **2013,** *4* (5), 847-851.